Nomination form for the 2020 Nishina Asia Award

Candidate (name, affiliation, curriculum vitae including the date of the degree of Ph.D., nationality, address, email and telephone)

Ssu-Yen Huang

CURRENT EMPLOYMENT

Associate Professor (2018-present)

Department of Physics, National Taiwan University

1, Sec. 4, Roosevelt Road, Taipei 10617, Taiwan

+886-2-3366-5179;

EDUCATION

Ph.D. (2003-2009) Electrophysics, National Chiao Tung University, Hsinchu, Taiwan.

M. S. (1999-2001) Physics, Fu Jen Catholic University, Taipei County, Taiwan

B. S. (1995-1999) Physics, Tamkang University, Taipei County, Taiwan

RESEARCH EXPERIENCE

2014-2018	Assistant Professor National Taiwan University
2013-2014	Postdoctoral Research Associate Johns Hopkins University
2011-2013	Postdoctoral Research Associate Dragon Gate Program at National Tsing Hua University, Taiwan and Johns Hopkins University.
2010-2011	Postdoctoral Research Associate Massachusetts Institute of Technology
2009-2010	Postdoctoral Research Associate Institute of Physics, Academia Sinica, Taipei, Taiwan

AWARDS

2018 Ta-You Wu Memorial Award

2018 and 2016 Outstanding Faculty Teaching Award

2018 Academia Sinica Junior Research Investigators Award.

2018 Research Achievement Award, Taiwan Association for Magnetic Technology.

2017 Ministry of Science and Technology "Excellent Young Scholar Research Program"

2015 Golden Jade Fellowship

2014 Asian Union of Magnetics Societies (AUMS) Young Researcher Award

2010 Ph. D. Dissertation award, The Physical Society of ROC

2009 Best Ph. D. dissertation award, Taiwan Association for Magnetic Technology.

Citation for the Award (within 30 words)
For his seminal contributions in pure spin current phenomena, including intrinsic spin-dependent thermal transport, spin Seebeck effect, transport magnetic proximity effect, inverse spin Hall effect, and spin-orbit torque in (anti)ferromagnets.

Description of the work

Energy dissipation is one of the toughest challenges for high-density electronic devices and a paramount issue in many emerging technologies. The recent advent of pure spin current with the attributes of maximal spin angular momentum and minimal charge current, thus least Joule heating, offers promising solutions to these problems. In the past years, Dr. Huang has been devoted to manipulating the polarized and pure spin currents associated with the spin caloritronic effects, such as the anomalous Nernst effect, spin Seebeck effect, and thermal Hall effect. He also has important contributions in studying the ferromagnetic resonance driven spin pumping, light-induced magnonic spin current, and current-induced *zero-field* spin-orbit torque effect in antiferromagnets. He has made many outstanding contributions and discoveries in this newly invigorated field, including one book chapter, 8 PRL, 14 PRB, 2 PRA, 1 PRM, 2APL, etc., which are cited more than 1900 times and lead to more than 25 invited talks in the important scientific conferences. Their impacts are briefly described as follows:

Spin Seebeck Effect: Spin caloritronics encompasses new effects that explore pure spin current phenomena and devices. Of those, the spin Seebeck effect (SSE) is one of the most important but inadequately established effects to generate pure spin current. The SSE exists in two configurations: transverse and longitudinal configurations with in-plane and out-of-plane temperature gradient, respectively. The first observations of the transverse SSE used thin ferromagnetic metals, semiconductors, and insulators deposited on thick substrates. Huang and his collaborators demonstrated experimentally that in such transverse SSE geometry, there is an unintentional temperature gradient perpendicular to the thin film due to the overwhelming thermal conduction through the substrate. As a result, the actual characteristics of the spin-dependent thermal transport are dominated by the anomalous Nernst effect (ANE) in ferromagnetic metals. This problem plagued many previous reports of the transverse SSE. Huang used substrate-free samples to demonstrate the intrinsic spin-dependent thermal transport in ferromagnets [Phys. Rev. Lett. **107**, 216604 (2011)], which has been *highlighted on Physics Synopsis* by the editor of Physical Review Letters. The longitudinal SSE geometry with an out-of-plane temperature gradient is applicable in generating spin current from ferromagnetic (FM) insulators such as yttrium iron garnet (YIG), and a nonmagnetic metal Pt on the FM insulator as in Pt/YIG is used as a spin current detector. Their results [Phys. Rev. Lett. **109**, 107204 (2012)] showed that although the temperature gradient $\nabla_z T$ is unequivocally out-of-plane, one encounters another issue of magnetic proximity effects (MPE) when Pt is in contact with an FM material. The magneto-transport measurements, both electrical and thermal, and evidences from x-ray magnetic circular dichroism results [Phys. Rev. Lett. **110**, 147207 (2013)], conclusively demonstrated the existence of MPE in Pt. Furthermore, Huang and his collaborators demonstrated a new type of magnetoresistance (MR) in Pt when it is in contact with an FM material. The new MR is distinctively different from all previous known MR effects, as described in [Phys. Rev. B **87** 220409(R) (2013)]. They showed different mechanisms that contribute to the new MR [Phys. Rev. Lett. **112**, 236601 (2014)], impacting the theoretical proposals for this MR. Most importantly, although many complications exist in the SSE systems, they demonstrated intrinsic longitudinal SSE without any appreciable MPE in Au/YIG [Phys. Rev. Lett. **110**, 067206 (2013)]. Their results have attracted a lot of attention. A more complete account of the SSE is in their book chapter [Solid State Physics **64**, 53 (2013)]. Beyond the YIG based system, they recently reported the first observation of SSE in highly spin-polarized ferromagnetic half metal LaSrMnO, which could be an important material for metal-based spin caloritronic devices in addition to FM insulators [Phys. Rev. B **96**, 00402(R) (2017)].

Spin Hall Materials: The most important quantity in pure spin current phenomena is the spin Hall angle (θ_{SH}), which measures the efficiency of charge/spin current conversion. There are several methods to determine θ_{SH}, including lateral spin valve, spin pumping, spin Hall switching and etc.. But each method has different complexities. The disparity in the values of θ_{SH} for the same material is one of the most outstanding issues in spin current phenomena. Huang and collaborators demonstrated a new and self-consistent method to determine θ_{SH} by employing a simple geometry of a metal/ferromagnetic insulator structure under a longitudinal thermal gradient and performed full spin current analyses of the inverse spin Hall voltage [Phys. Rev. B **89**, 140407(R) (2014)]. Huang further showed that this method, which uses the SSE to generate spin current, is robust and does not depend on the crystallinity of the spin current generator YIG [Phys. Rev. Materials **1**, 031401(R) (2017)]. While the spin Hall property is intrinsic for given material, recently, they showed that both the θ_{SH} and spin Hall conductivity in AuTa alloy exhibit a quasilinear dependence on its composition, demonstrating the importance of conduction electrons over band structures in determining the θ_{SH} for binary alloys [Phys. Rev. B **97**, 024402 (2018)]. In addition, they achieved utilizing the spin current to probe the spin frustrations and spin fluctuations in spin glass $Cu_{1-x}Mn_x$ alloys [Phys. Rev. B **101**, 104413 (2020)]. And they observed that spin current can be significantly enhanced during the spin-freezing process. Their results provide important guidance in materials engineering for future spintronic devices.

Spin Hall effect and Spin-Orbit Torque in Ferromagnet and antiferromagnet: Inverse spin Hall effect has been established only in non-magnetic metals (e.g., Pt, W) with strong spin-orbit coupling (SOT) for a long time. Huang and collaborators reported the first observation of the inverse spin Hall effect in a 3*d ferromagnetic* metal of permalloy (Py) [Phys. Rev. Lett. **111**, 066602 (2013)]. This is the inverse effect of the well-known anomalous Hall effect in ferromagnetic metals. Ferromagnetic materials not only can generate spin-polarized current but also can be used to detect pure spin current. The large θ_{SH} in Py indicates that many other ferromagnetic metals can be exploited for pure spin current applications. These important results have been selected as the *Editors' suggestion* in Physical Review Letters. Besides ferromagnets, Huang and collaborator also found that chromium (Cr), which is a *3d* spin-density wave antiferromagnetic metal, has a large inverse spin Hall effect below and above its phase transition temperature [Phys. Rev. B. **92**, 020418 (R) (2015)]. This result leads to another important breakthrough, *field-free spin-orbit torque (SOT) switching* in heavy-metal-free Cr-based heterostructures [Phys. Rev. Applied **11**, 061005 (2019) (Letter)]. Moreover, they demonstrated the high-entropy alloy can also generate sizable spin-orbit torques for FM switching [Phys. Rev. Applied **8**, 044005 (2017)]. Very recently, Huang made an important contribution to the SOT antiferromagnetic (AFM) Néel vector switching. Antiferromagnet with zero net magnetization has several unique advantages, including ultrafast dynamics in the terahertz frequencies, robustness against field perturbation, and negligible stray field. Recently, there have been numerous reports of electrical switching of AFM Néel vector via SOT, attracting worldwide attention. By applying a writing current in the AFM layer or the normal metal (NM)/AFM bilayer, in a patterned multiterminal device, the measured resistance exhibited recurring signals due to the supposedly electrical switching of the AFM Néel vector. However, Huang showed that under a large writing current density beyond the Ohmic regime, the multiterminal devices generate unintended anisotropic thermal gradients and voltages [Phys. Rev. Lett. **123**, 227203 (2019)]. Thus, this widely held switching signal may not be the conclusive evidence of SOT switching of AFM but the thermal artifacts of patterned metal structures on substrates. Similar signals can be observed in such patterned structures, with and without the AFM layer. Consequently, the strength of the signal is greatly affected by the thermal conductivity of the substrates. This important observation is *highlighted by Physic Review Letters' Editors* as *Editors' suggestion and Featured in Physics* with a "Viewpoint: The heat in antiferromagnetic switching".

Thermal spin current to explore surface magnetization: Huang showed that the thermal measurement with a vertical temperature gradient could be an important tool for detecting magnetization structure with high sensitivity [Phys. Rev. B. **94**, 024405 (2016)]. By using thermal spin current and highly sensitive micro-magneto-optic Kerr effect (MOKE) measurements, he conclusively showed that the peculiar field dependence of the thermal voltage is due to the noncollinear magnetization between the surface and bulk YIG. Huang further experimentally demonstrated that the contributions of the interfacial and bulk temperature gradients in spin caloritronics can be revealed by the light excited thermal spin current measurement [Phys. Rev. B **99**, 094426 (2019)]. By flipping the direction of the incident light, the interfacial and bulk contributions to the transverse spin accumulation he can be qualitatively distinguished for the first time. Huang showed that the derived interfacial and bulk spin Seebeck coefficient is intrinsic and frequency-independent. Thus, unlike conventional electrical heating, light offers distinct heating mechanism to develop spintronic and spin caloritronic devices.

Thermal excited spin-polarized current: Huang designed several unique measurement configurations to distinguish the contributions of the spin-dependent thermal voltages from the thermal Hall effect (THE), the anomalous Nernst effect (ANE), and the spin Seebeck effect (SSE) in [Phys. Rev. Lett. **117**, 247201 (2016)]. Although recent theoretical researches indicate that the THE can compromise the legitimacy of all thermal related spin physics effects in spin caloritronics, Huang experimentally demonstrated that these speculations are false. He confirmed that ANE and SSE are indispensable tools to explore thermal spin current. Moreover, they showed in [Phys. Rev. B **96**, 174406 (2017)] that the ANE is thickness dependent. They found that the magnitude and even sign of the ANE exhibit nontrivial thickness-dependent behaviors in conventional FMs, including Fe, Co, Ni, and Py. Most importantly, the conversion efficiency of the spin signals generated by heat flows can be significantly enhanced to one order of magnitude in ultra-thin films. They demonstrated that this enhancement is dominated by the intrinsic Berry curvature and side-jump mechanisms. These findings also reveal various potential applications of spin-based thermoelectrics for energy harvesting.

Incoherent spin pumping: Although the spin pumping (SP) and the SSE, two of the most common methods for generating pure spin currents from ferromagnetic insulators, are considered to share similar physical mechanisms, Huang showed that while the SP is significantly reduced in a polycrystalline yttrium iron garnet (YIG), the SSE is insensitive to the crystalline structures [Phys. Rev. Materials **1**, 031401(R) (2017)]. This discovery offers new insights into the mechanisms between the coherently driven SP and the non-coherently excited SSE. This work is *highlighted by Physical Review Editors* and introduced by editors of Nature publisher as a research *highlight article* in *Nature Nanotechnology* [Nat. Nanotech. **12**, 936 (2017)]. Very recently, they further showed that the evidence is absent for coherent spin pumping in Pt/YIG [Phys. Rev. B **99**, 220402 (R) (2019)]. When YIG samples of an appropriate thickness has been used, all the spin wave resonance modes can be resolved and their temperature dependence and that of coherent spin pumping can be separately followed. They showed that there is *no* evidence of coherent spin pumping, which was expected to prevail at low temperatures. These are some of the most essential questions in pure spin current phenomena to date.

Dr. Huang and his collaborators' works have a profound and high impact on both fundamental physics and applications of spin-based phenomena in the emerging field of spin caloritronics and spintronics. Their papers have been heavily cited and thus far have led to 25 invited talks in the important scientific meetings. Dr. Huang has been awarded the Ta-You Wu Memorial Award and Academia Sinica Junior Research Investigators Award in 2018, Golden Jade Fellowship in 2015, AUMS Young Researcher Award in 2014. He is distinctly qualified for the 2020 Nishina Asia Award.

Key references (up to 3 key publications*)

1. C. C. Chiang, S. Y. Huang*, D. Qu, P. H. Wu, C. L. Chien, "*Absence of evidence of electrical switching of the antiferromagnetic Néel vector*", Phys. Rev. Lett., **123**, 227203 (2019) (Editors' suggestion and Featured in Physics). Viewpoint on Physics: The heat in antiferromagnetic switching.
2. S. Y. Huang*, X. Fan, D. Qu, Y. P. Chen, W. G. Wang, J. Wu, T. Y. Chen, J. Q. Xiao and C. L. Chien, *Transport magnetic proximity effects in platinum*, Phys. Rev. Lett. **109**, 107204 (2012).
3. S. Y. Huang*, W. G. Wang, S. F. Lee, J. Kwo, and C. L. Chien, *Intrinsic spin-dependent thermal transport*, (2011) Phys. Rev. Lett. **107**, 216604. *Editor highlights* on Physics Synopsis.

*) Copy of one most significant publication should be attached.

Nominator (name, affiliation, email, telephone and relation to the candidate)

Prof. Yuan-Huei Chang

Department of Physics, National Taiwan University

Email: yhchang@phys.ntu.edu.tw

Relation to the candidate: colleague and former department chair

Signature Yuan Huei Chang Date 2020-03-30

PHYSICAL REVIEW LETTERS
moving physics forward

Dear Sir or Madam,

We are pleased to inform you that the Letter

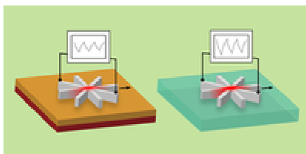

Absence of evidence of electrical switching of the antiferromagnetic Néel vector

C.C. Chiang *et al.*
Phys. Rev. Lett. **123**, 227203 (2019)

Published 27 November 2019

has been highlighted by the editors as an Editors' Suggestion. Publication of a Letter is already a considerable achievement, as *Physical Review Letters* accepts fewer than 1/4 of submissions, and is ranked first among physics and mathematics journals by the Google Scholar five-year h-index. A highlighted Letter has additional significance, because only about one Letter in six is highlighted as a Suggestion due to its particular importance, innovation, and broad appeal. Suggestions are downloaded twice as often as the average Letter, and are covered in the press substantially more often. If Suggestions were a separate publication, they would have an Impact Factor of 17. More information about our journal and its history can be found on our webpage prl.aps.org.

Yours sincerely,

Hugues Chaté
Editor
Physical Review Letters

Michael Thoennessen
Editor in Chief
Physical Review

Editors' Suggestion Featured in Physics

Absence of Evidence of Electrical Switching of the Antiferromagnetic Néel Vector

C. C. Chiang,[1] S. Y. Huang,[1,*] D. Qu,[2] P. H. Wu,[1] and C. L. Chien[1,2,3]
[1]*Department of Physics, National Taiwan University, Taipei 10617, Taiwan*
[2]*Institute of Physics, Academia Sinica, Taipei, 11529, Taiwan*
[3]*Department of Physics and Astronomy, Johns Hopkins University, Baltimore, Maryland 21218, USA*

(Received 23 July 2019; revised manuscript received 16 September 2019; published 27 November 2019)

Much theoretical and experimental attention has been focused on the electrical switching of the antiferromagnetic (AFM) Néel vector via spin-orbit torque. Measurements employing multiterminal patterned structures of Pt/AFM show recurring signals of the supposedly planar Hall effect and magnetoresistance, implying AFM switching. We show in this Letter that similar signals have been observed in structures with and *without* the AFM layer, and of an even larger magnitude using different metals and substrates. These may not be the conclusive evidence of spin-orbit torque switching of AFM, but the thermal artifacts of patterned metal structure on substrate. Large current densities in the metallic devices, beyond the Ohmic regime, can generate unintended anisotropic thermal gradients and voltages. AFM switching requires unequivocal detection of the AFM Néel vector before and after SOT switching.

DOI: 10.1103/PhysRevLett.123.227203

Purely electrical control of magnetic devices is an ultimate goal in spintronics. Previously, spin transfer torque (STT) could provide electrical switching of ferromagnetic (FM) layers but required at least two FM entities, e.g., Co/Cu/Co, where the spin-polarized current from one FM switches the magnetization of the other FM [1]. The recent discovery of spin-orbit torque (SOT) accommodates electrical switching of a single FM layer adjacent to a heavy metal (HM), such as in HM/FM bilayers [2–4]. Spin-orbit torque (SOT) switching is based on the spin Hall effect, where a charge current through the HM (e.g., Pt) with a large spin Hall angle θ_{SH} generates a pure spin current in the lateral direction with the spin index σ in the third direction. Above a threshold current density, the SOT can electrically switch the adjacent FM with in-plane anisotropy as well as perpendicular magnetic anisotropy, but the latter requires an external field along the current direction, and is thus highly undesirable. Several schemes have been demonstrated to achieve field-free SOT switching of the FM layer with perpendicular magnetic anisotropy [5–12].

It has been well established in both STT and SOT that switching of the magnetization $\boldsymbol{M}$ of an FM layer occurs *only* when the current density j has exceeded the critical value j_c [1–12]. There is no appreciable change of $\boldsymbol{M}$ at $j < j_c$, regardless of the duration of the current or the number of such current pulses. Only until $j \geq j_c$, swift and irreversible changes in $\boldsymbol{M}$ occur. Switching (or lack thereof) can be readily revealed by the measurement of $\boldsymbol{M}$ using magnetometry, or more simply, by suitable Hall effect and magnetoresistance (MR). The evidence for switching is unequivocal and can be readily verified by rotating $\boldsymbol{M}$ of the FM via a small magnetic field to the specific directions.

The recent proposal of electrical switching via SOT of the antiferromagnetic (AFM) materials, with the potential of ushering in AFM spintronics with terahertz frequencies, has attracted much attention [13–18]. However, unlike FMs, AFMs have no net magnetization ($\boldsymbol{M} = 0$). They are weakly responsive to magnetic field, but display a rich variety of AFM spin structures from uniaxial to kagome lattice. Most theoretical and experimental studies of AFM switching have focused on the simplest AFMs with two colinear sublattice magnetizations in opposite directions $\boldsymbol{M_1} = -\boldsymbol{M_2}$ defining a Néel vector $\boldsymbol{n}_{\mathrm{N\acute{e}e}l=(\boldsymbol{M_1}-\boldsymbol{M_2})/2M_0}$, where M_0 is the magnitude of the sublattice magnetization. Theories suggest that the antidamping SOT, but not the fieldlike SOT, can switch the AFM Néel vector $\boldsymbol{n}_{\mathrm{N\acute{e}el}}$ with $\boldsymbol{M} = 0$ [19]. However, ascertaining electrical switching of the AFM Néel vector remains a formidable challenge, compounded by the fact that most AFMs have no well-defined $\boldsymbol{n}_{\mathrm{N\acute{e}el}}$.

Experimental exploration of AFM switching was first reported in epitaxial thin films of CuMnAs, an unusual metallic AFM with broken inversion symmetry [13]. As such, it is argued that CuMnAS (a similar situation also exists in $\mathrm{Mn_2Au}$) affords Néel SOT switching without the necessity of an adjacent HM layer [13–15]. Most AFM switching studies have used Pt/NiO, where the SOT from Pt may switch NiO [16–18], a well-known AFM insulator. It has been assumed in the AFM switching studies that the AFM thin films would acquire the same AFM spin structures as those in bulk crystals, a premise that has not been borne out in extensive studies of exchange bias, which also involves AFM thin films [20].

To detect AFM switching, most studies have employed multiterminal structures, such as the four-terminal or the eight-terminal patterned structure. The eight-terminal

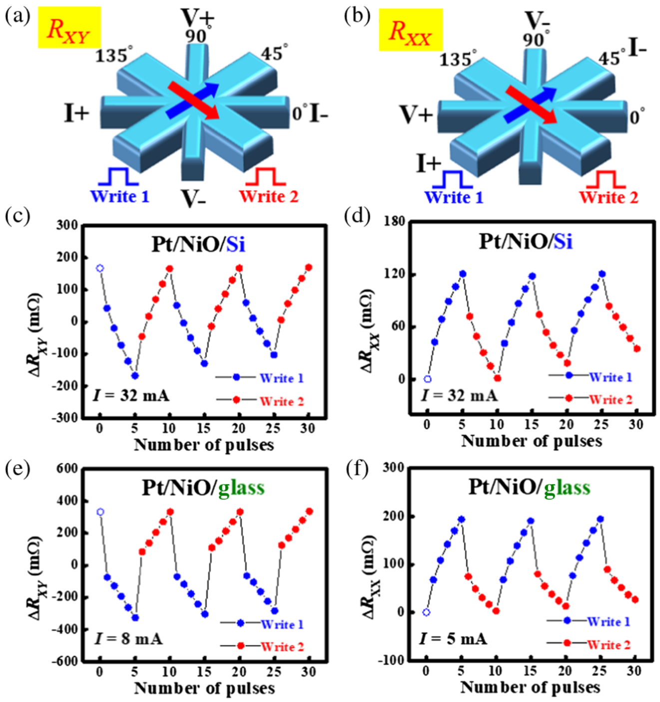

FIG. 1. Schematics of the eight-terminal patterned structure with the pulsed writing current along the 45° (write 1) and the 135° (write 2) lines for (a) planar Hall and (b) longitudinal resistance measurements. Relative changes of Hall resistance (ΔR_{XY}) in (c) Pt/NiO/Si and (e) Pt/NiO/glass and relative change of longitudinal resistance (ΔR_{XX}) in (d) Pt/NiO/Si and (f) Pt/NiO/glass, after applying 10-ms writing current pulses alternately along the 45° and the 135° lines.

structure, consisting of four electrical lines oriented at 0°, 45°, 90°, and 135°, is intended to capture the planar Hall effect (PHE) resistance R_{XY} in Fig. 1(a) and the MR resistance R_{XX} in Fig. 1(b) after the large writing current 1 (blue) and 2 (red) (along the 45° or 135° lines) switches the AFM Néel vector. The reading current and the measured voltage for both R_{XY} and R_{XX} are marked by $I+$, $I-$, $V+$, and $V-$ in Figs. 1(a) and 1(b). The MR may be the anisotropic MR in metallic AFMs [13–15] or the spin Hall MR in Pt/AFM bilayers [16–18,21–23]. We used the same patterned eight-terminal structure and obtained the same qualitative results as those in CuMnAS and Mn_2Au without HM, and in Pt/NiO. The crucial questions are whether or not these are evidence for SOT switching of the AFM Néel vector.

We use the *same* Pt(4)/NiO(60) bilayers, where polycrystalline 4 nm Pt and 60 nm NiO bilayers have been made by magnetron sputtering, onto substrate and patterned into the same eight-terminal devices with 20-μm wide writing leads along the 45° and the 135° directions, and 10-μm wide reading leads along the 0° and the 90° directions for R_{XY} and R_{XX}. For example, a writing current of 32 mA through the 20-μm wide Pt (4 nm) gives a current density of 4×10^7 A/cm^2. We use pulsed writing currents of magnitude I with the same pulse width of 10 ms. After a 10-s delay time, the resistances R_{XY} and R_{XX} are subsequently measured at a much lower current density of 2.5×10^5 A/cm^2 from the reading leads. Our results of R_{XY} and R_{XX} of Pt(4)/NiO(60)/Si are shown in Figs. 1(c) and 1(d), respectively. They are expressed as the relative changes of Hall resistance ΔR_{XY} and longitudinal resistance ΔR_{XX}, where ΔR_{XY} steadily decreases (increases) with the number of writing current 1 blue (2 red) pulses of 32 mA along the 45° (135°) line, and ΔR_{XX} changes oppositely. The recurring results of ΔR_{XY} and ΔR_{XX} between write currents 1 and 2, very similar to those observed in CuMnAS, Pt/NiO, and Mn_2Au, have previously been claimed as evidence of SOT switching of AFMs [13–18]. However, these highly unusual results warrant closer analyses.

First of all, the results in Figs. 1(c) and 1(d) show that each current pulse of writing current 1 (blue) creates essentially the *same* incremental change in ΔR_{XY} and ΔR_{XX}. If these were related to AFM switching, it would imply that each current pulse would create a small but similar Néel vector rotation and/or AFM domain reversal. The extent of AFM switching would scale with the *number* of pulses, i.e., more pulses would cause a larger portion of switching. Reverting to writing current 2 (red), each current pulse would create the *same* but *reversed* incremental change in AFM switching. These behaviors, if indeed due to AFM switching, would be diametrically different from those known in SOT or STT switching of FM systems, where, at $j < j_c$, there are no incremental changes, nor reversed incremental changes, nor accumulative changes of magnetization reversal at all [1–12].

It is also important to stress the large writing current of 32 mA with a high current density of 4×10^7 A/cm^2 in Figs. 1(c) and 1(d). At $I < 25$ mA, we obtained only $R_{XY} \approx 0$ and $\Delta R_{XY} \approx 0$; $R_{XX} \approx$ constant and $\Delta R_{XX} \approx 0$. Only with a larger current, e.g., 32 mA, could we measure appreciable R_{XY}, ΔR_{XY}, and ΔR_{XX}, the size of which *scales* with the write current I. At a slightly higher current of $I \approx 35$ mA the sample was destroyed. We illustrate these aspects with another nominally the same Pt(4)/NiO(60)/Si sample from low current to the breakdown current using one-shot pulses, as shown in Fig. 2. Below 25 mA, $R_{XY} \approx 0$ and $\Delta R_{XY} \approx 0$; $R_{XX} \approx 90.6\ \Omega$ and $\Delta R_{XY} \approx 0$, and these values are independent of I. This is the Ohmic regime, in which the voltage is linearly proportional to current yielding a constant resistance independent of current. The Ohmic regime is where resistance measurements of any metal are normally made, with a lower current to avoid excessive joule heating. The results of $R_{XY} \approx 0$ and $\Delta R_{XY} \approx 0$ indicate there is no PHE signal, i.e., no evidence of AFM switching.

However, at $I > 25$ mA, R_{XY} and R_{XX} rise sharply with I, as shown in Figs. 2(a) and 2(c), respectively, i.e., highly non-Ohmic, and at 42 mA the device breaks down. Only in the non-Ohmic regime with a very high current can one observe the sizable changes for ΔR_{XY} and ΔR_{XX} on pulse

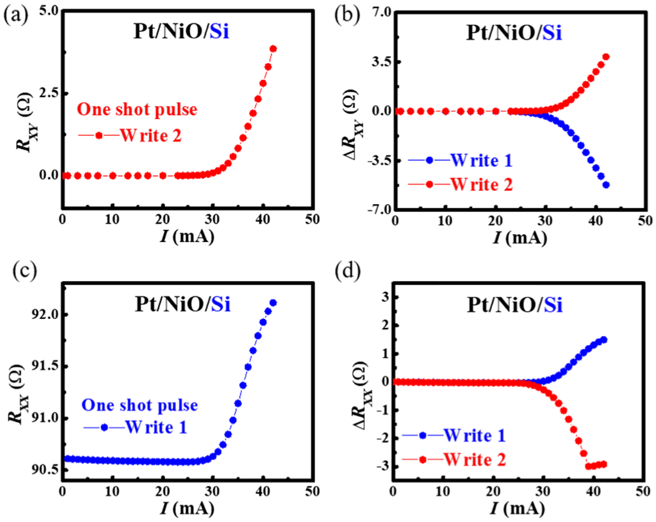

FIG. 2. (a) R_{XY} and (b) ΔR_{XY} in Pt/NiO/Si as a function of one-shot writing current pulses along the 45° (write 1) or the 135° (write 2) lines. (c) R_{XX} and (d) ΔR_{XX} in Pt/NiO/Si as a function of one-shot current pulse along the 45° (write 1) or the 135° (write 2) lines.

writing current with different orientations, as shown in Fig. 2(b). The values of R_{XX}, ΔR_{XX}, R_{XY}, and ΔR_{XY} are not constant but rise sharply with I. Thus, the evidence of AFM switching to date, the increasing and decreasing ΔR_{XY}, could just be the result of the resistance measurements in the non-Ohmic regime at very high current density, below the breakdown current. The high current density exceeding 10^7 A/cm^2 also develops serious thermal issues with irreversible damages due to intense heat and electromigration. After such high current densities, the resistance of the metallic device has suffered permanent changes.

Since R_{XY} and R_{XX} are electrical characteristics, one expects the results to be intrinsic to Pt(4)/NiO(60) and independent of the insulating substrate on which the patterned Pt(4)/NiO(60) structures are situated. Quite the contrary, we found both R_{XY} and R_{XX} depend greatly on substrates. The results of the same patterned structures on glass, as shown in Figs. 1(e) and 1(f), are much larger than those on Si, with those on MgO in between (not shown). This indicates a strong influence of substrate for electrical measurements at very high current density, in particular, the heat dissipation through the substrate. The larger ΔR_{XY} and ΔR_{XX} for structures on glass, as compared to those on Si, are due to the lower thermal conductivity κ of glass as shown in Table I. Therefore, the same structures when patterned on glass substrate exhibit similar signals but of far greater magnitude. Note that the writing current in Pt/NiO/glass [Fig. 1(e)] is only 8 mA, but the values of ΔR_{XY} are much larger than those for Pt/NiO/Si [Fig. 1(c)] at 32 mA. Likewise, the ΔR_{XX} for Pt/NiO/glass shown in Fig. 1(f) at 5 mA are much larger than those for Pt/NiO/Si at 32 mA shown in Fig. 1(d). Because of the much lower κ for glass, Pt/NiO/glass also has a much lower onset current for the non-Ohmic regime and breakdown current than those for Pt/NiO/Si. Since only the writing current dictates the strength of the SOT that switches the Néel vector of the AFM NiO, the large variations in ΔR_{XX}, ΔR_{XY}, and the onset writing current due to different substrates strongly indicate these are not evidence of SOT switching of the AFM Néel vector.

TABLE. I. Thermal conductivity of Si, MgO, and glass [24]. Simulation of rising temperature in Pt (4 nm) on Si, MgO, and glass and temperature difference between T_1 and T_2 in Fig. 4(a), after applying one-shot writing current of density of 1.75×10^7 A/cm^2.

Substrate	Thermal conductivity (W/mK)	T_1 (K)	T_2 (K)	ΔT (K)
Silicon	131	301.25	301.36	0.11
MgO	30	304.92	305.38	0.46
Glass	1.38	383.64	393.78	10.14

We further patterned the same eight-terminal structure on Si, MgO, and glass with only the metal Pt and *without* the AFM layer of NiO, thus removing any possibility of AFM switching. Still, the *same* sawtooth recurring patterns in ΔR_{XY} and ΔR_{XX} can be observed, as shown in Fig. 3. These signals, without NiO, increase in the order of Pt/Si, Pt/MgO, and Pt/glass, reflecting the thermal conductivity of the substrates, and illustrating that these recurring results are non-Ohmic joule heating in Pt only. Thus, the recurring sawtooth signals in Pt/NiO are unrelated to SOT AFM switching.

The eight-terminal devices were designed to exploit the PHE and MR to reveal the SOT switching of the AFM Néel vector. While the PHE and MR are established methods for

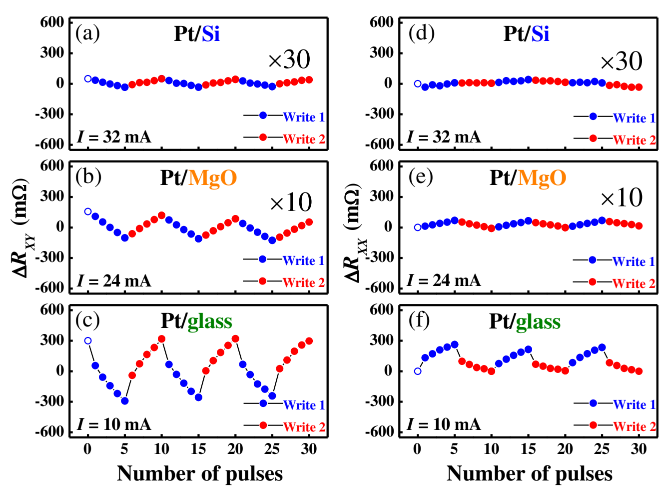

FIG. 3. The values of ΔR_{XY} and ΔR_{XY} after applying successive writing pulses current alternately along the 45° and the 135° lines for (a) Pt/Si, (b) Pt/MgO, and (c) Pt/glass; and for (d) Pt/Si, (e) Pt/MgO, and (f) Pt/glass, respectively, without any AFM.

detecting the direction of $\boldsymbol{M}$ of the FM layer, they have never been demonstrated for detecting the Néel vector of an AFM layer, for there is no simple method to create and orient the AFM Néel vector to the specific directions on demand. Unfortunately, the eight-terminal patterned structure also creates unforeseen complications in electrical measurements. The eight terminals are connected to the same *common* area, which receives the writing current of a large current density and whose electrical characteristics are subsequently measured to assess possible AFM switching. The intended PHE and MR results inadvertently include unintended contributions of the asymmetrical temperature gradient, thermal voltages, and Hall voltages.

Only a high writing current beyond the Ohmic regime, with a current density in the $10^7\ \mathrm{A/cm^2}$ range, generates measurable values of R_{XY} and ΔR_{XY}. After the application of a writing current 1 (blue) pulse, there is a large temperature rise in the 45° line, by more than 100 K, as corroborated by the COMSOL simulation as shown in Figs. 4(a) and 4(c), which creates a net temperature gradient between the voltage leads in the 90° line. For the R_{XY} measurements, the current and voltage leads are along the 0° and the 90° lines, respectively. This leads to the Seebeck effect in the direction of the temperature gradient. Any metal (e.g., Pt, Cr, and Au) with a significant Seebeck effect gives rise to a thermal voltage with an increasing magnitude

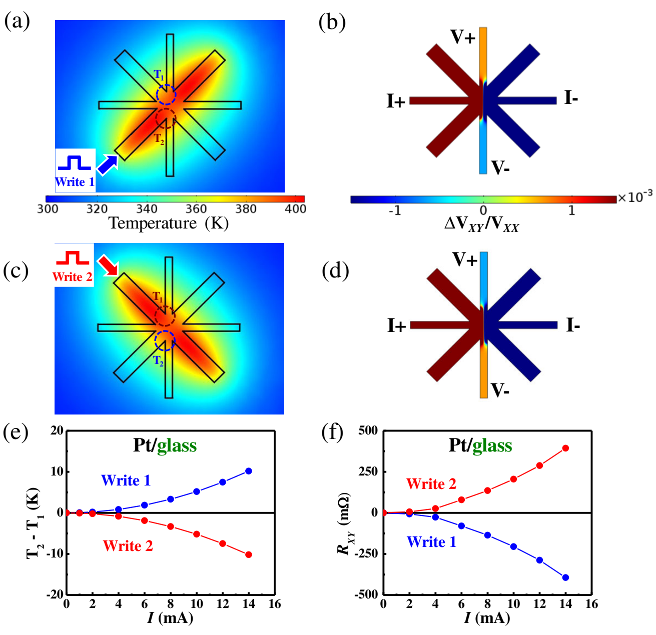

FIG. 4. Simulation of temperature distribution for the eight-terminal patterned Pt/glass structure after applying one-shot current of density $1.75 \times 10^7\ \mathrm{A/cm^2}$ along (a) 45° (write 1) and (c) 135° (write 2) lines. Simulation of Hall signal induced after one-shot writing current along (b) 45° (write 1) and (d) 135° (write 2) lines with the relative Seebeck coefficient of 8 μV/K. (e) The temperature difference between T_1 and T_2 and (f) R_{XY} as a function of one-shot current pulse along 45° (write 1) and (c) 135° (write 2) lines.

for each successive writing current 1 (blue) pulse. When one reverts to the writing current 2 (red), the 135° line is heated. As compared with Figs. 4(b) and 4(d), the temperature gradient between the voltage leads in the 90° line now reverses to give an opposite sign of thermal voltage, that increases with each of the successive writing current pulses. The simulation values are qualitatively consistent with experiments with a relative Seebeck coefficient around 8 μV/K [25,26]. These temperature differences and voltages scale sharply with the current as shown in Figs. 4(e) and 4(f), giving the appearance of recurring Hall resistance signals, by the same token, the MR voltage as well, as shown in Supplemental Material Fig. S1 [27]. In addition to Pt, we have also patterned Cr and Au. As shown in Supplemental Material Fig. S2 [27], the signals for Cr are much larger than those of Pt and Au because of the larger Seebeck coefficient of Cr [29]. These thermal voltages, intrinsic to the metal layer of Pt, Au, and Cr, have nothing to do with AFM switching.

Previous studies of AFM switching have noted the intense heat in the device [30,31]. Some protocols, e.g., a pause of 10 s after the writing current pulse before the electrical measurements, have been used to alleviate the heating problem. Our measurements reveal that 10 s is far too short for the intense heat to dissipate. In fact, we have found a sizable $\boldsymbol{\Delta} R_{XY}$ and temperature gradient remains in the patterned structures even after one hour. Very high current density may also anneal the thin films, cause electromigration and other irreversible damages, causing permanent changes of the resistance, as shown in Supplemental Material Fig. S2 [27]. Furthermore, after the sample has been subjected to a high writing current pulse, subsequent measurements at a lower current may reveal a sawtooth of different magnitudes, and in some cases, even altering the sawtooth shape into steplike signals [32], as illustrated in Supplemental Material Fig. S3 [27]. Recent experiments also indicate a non-spin-torque origin of AFM switching [33].

In summary, much attention has been focused recently on SOT switching of AFM Néel vector employing multiterminal patterned structures that show recurring signals in PHE ΔR_{XY} and MR ΔR_{XX} signals. We show in this work that these voltage and resistance signals may not be conclusive evidence of SOT switching of AFM, but the artifacts of the large writing currents beyond the Ohmic regime through the metallic multiterminal devices. The prospect of SOT switching of AFM Néel vector encounters numerous challenges. Many AFMs have complex spin structures without a well-defined Néel vector. Even for AFMs that may accommodate a Néel vector, it remains a challenge to unequivocally detect the AFM Néel vector, before and after the SOT switching.

This work was supported by the Ministry of Science and Technology of Taiwan, under the Grant No. MOST 106-2628-M-002-015-MY3. This work was also partially supported by Academia Sinica and National Taiwan University. We thank D. Y. Kang and C. T. Chen from National Taiwan University for simulation support. Work at JHU was supported by KAUST (Grant No. OSR2017-CRG6-3427.01) and the U.S. Department of Energy (Award No. DE-SC0009390 and No. SC0012670).

*syhuang@phys.ntu.edu.tw

[1] E. B. Myers, D. C. Ralph, J. A. Katine, R. N. Louie, and R. A. Buhrman, Science **285**, 867 (1999); D. C. Ralph and M. D. Stiles, J. Magn. Magn. Mater. **320**, 1190 (2008).
[2] L. Liu, C. F. Pai, Y. Li, H. W. Tseng, D. C. Ralph, and R. A. Buhrman, Science **336**, 555 (2012).
[3] I. M. Miron, K. Garello, G. Gaudin, P. J. Zermatten, M. V. Costache, S. Auffret, S. Bandiera, B. Rodmacq, A. Schuhl, and P. Gambardella, Nature (London) **476**, 189 (2011).
[4] L. Liu, O. J. Lee, T. J. Gudmundsen, D. C. Ralph, and R. A. Buhrman, Phys. Rev. Lett. **109**, 096602 (2012).
[5] G. Yu, P. Upadhyaya, Y. Fan, J. G. Alzate, W. Jiang, K. L. Wong, S. Takei, S. A. Bender, L. T. Chang, Y. Jiang, M. Lang, J. Tang, Y. Wang, Y. Tserkovnyak, P. K. Amiri, and K. L. Wang, Nat. Nanotechnol. **9**, 548 (2014).
[6] L. Youa, O. Leea, D. Bhowmika, D. Labanowskia, J. Honga, J. Bokora, and S. Salahuddin, Proc. Natl. Acad. Sci. U.S.A. **112**, 10310 (2015).
[7] Y. W. Oh, S. H. Chris Baek, Y. M. Kim, H. Y. Lee, K. D. Lee, C. G. Yang, E. S. Park, K. S. Lee, K. W. Kim, G. Go, J. R. Jeong, B. C. Min, H. W. Lee, K. J. Lee, and B. G. Park, Nat. Nanotechnol. **11**, 878 (2016).
[8] S. Fukami, C. Zhang, S. DuttaGupta, A. Kurenkov, and H. Ohno, Nat. Mater. **15**, 535 (2016).
[9] A. van den Brink, G. Vermijs, A. Solignac, J. Koo, J. T. Kohlhepp, H. J. Swagten, and B. Koopmans, Nat. Commun. **7**, 10854 (2016).
[10] Q. Ma, Y. Li, D. B. Gopman, Y. P. Kabanov, R. D. Shull, and C. L. Chien, Phys. Rev. Lett. **120**, 117703 (2018).
[11] S. C. Baek, V. P. Amin, Y. W. Oh, G. Go, S. J. Lee, G. H. Lee, K. J. Kim, M. D. Stiles, B. G. Park, and K. J. Lee, Nat. Mater. **17**, 509 (2018).
[12] T. C. Chuang, C. F. Pai, and S. Y. Huang, Phys. Rev. Applied **11**, 061005 (2019).
[13] P. Wadley *et al.*, Science **351**, 587 (2016).
[14] S. Yu. Bodnar, L. Šmejkal, I. Turek, T. Jungwirth, O. Gomonay, J. Sinova, A. A. Sapozhnik, H.-J. Elmers, M. Kläui, and M. Jourdan, Nat. Commun. **9**, 348 (2018).
[15] X. F. Zhou, J. Zhang, F. Li, X. Z. Chen, G. Y. Shi, Y. Z. Tan, Y. D. Gu, M. S. Saleem, H. Q. Wu, F. Pan, and C. Song, Phys. Rev. Applied **9**, 054028 (2018).
[16] X. Z. Chen, R. Zarzuela, J. Zhang, C. Song, X. F. Zhou, G. Y. Shi, F. Li, H. A. Zhou, W. J. Jiang, F. Pan, and Y. Tserkovnyak, Phys. Rev. Lett. **120**, 207204 (2018).
[17] T. Moriyama, K. Oda, T. Ohkochi, M. Kimata, and T. Ono, Sci. Rep. **8**, 14167 (2018).
[18] L. Baldrati, O. Gomonay, A. Ross, M. Filianina, R. Lebrun, R. Ramos, C. Leveille, T. Forrest, F. Maccherozzi, E. Saitoh, J. Sinova, and M. Kläui, arXiv:1810.11326v1.
[19] V. Baltz, A. Manchon, M. Tsoi, T. Moriyama, T. Ono, and Y. Tserkovnyak, Rev. Mod. Phys. **90**, 015005 (2018).
[20] J. Nogué and I. K. Schuller, J. Magn. Magn. Mater. **192**, 203 (1999).
[21] G. R. Hoogeboom, A. Aqeel, T. Kuschel, T. T. M. Palstra, and B. J. van Wees, Appl. Phys. Lett. **111**, 052409 (2017).
[22] J. Fischer, O. Gomonay, R. Schlitz, K. Ganzhorn, N. Vlietstra, M. Althammer, H. Huebl, M. Opel, R. Gross, S. T. B. Goennenwein, and S. Geprägs, Phys. Rev. B **97**, 014417 (2018).
[23] L. Baldrati, A. Ross, T. Niizeki, C. Schneider, R. Ramos, J. Cramer, O. Gomonay, M. Filianina, T. Savchenko, D. Heinze, A. Kleibert, E. Saitoh, J. Sinova, and M. Kläui, Phys. Rev. B **98**, 024422 (2018).
[24] S. Y. Huang, D. Qu, and C. L. Chien, *Charge, Solid State Physics* (Academic Press, Oxford, 2013), Vol. 64, pp. 53–82.
[25] Y.-J. Chen and S.-Y. Huang, Phys. Rev. Lett. **117**, 247201 (2016).
[26] T. C. Chuang, P. L. Su, P. H. Wu, and S. Y. Huang, Phys. Rev. B **96**, 174406 (2017).
[27] See Supplemental Material at http://link.aps.org/supplemental/10.1103/PhysRevLett.123.227203 for more details on COMSOL simulations for eight and four terminal devices, the time dependent Hall resistance with different substrates and normal metals, and the evolution between the sawtooth and the steplike switching behaviors, which includes Ref. [27].
[28] G. A. Slack, J. Appl. Phys. **35**, 339 (1964).
[29] W. M. Haynes, *CRC Handbook of Chemistry and Physics* (CRC Press, Oakville, 2014), 95th ed.
[30] M. Meinert, D. Graulich, and T. Matalla-Wagner, Phys. Rev. Applied **9**, 064040 (2018).
[31] T. Matalla-Wagner, M.-F. Rath, D. Graulich, J.-M. Schmalhorst, G. Reiss, and M. Meinert, arXiv:1903.12387.
[32] Y. Cheng, S. Yu, M. Zhu, J. Hwang, and F. Yang, arXiv:1906.04694.
[33] P. Zhang, J. Finley, T. Safi, J. Han, and L. Liu, arXiv:1907.00314.

VIEWPOINT

The Heat in Antiferromagnetic Switching

New experiments suggest that heat might be responsible for the current-induced voltage signals measured in antiferromagnets, and not a rotation of the material's spins as previously thought.

by Barry Zink*

Ferromagnets—magnetic materials in which the spins of neighboring atoms align—form permanent magnets whose "sticky" properties have been exploited in technologies for millennia. But their close magnetic cousins the antiferromagnets, materials in which neighboring spins point in opposite directions, have yet to find practical use. This lack of use most likely arises from their pattern of alternating spins, which ties the magnetic flux up inside the material, making its magnetism difficult to detect and manipulate. Scientists are now developing so-called all-electrical methods to control antiferromagnets; these techniques may finally change this status quo. But new measurements from Chih-Chieh Chiang from National Taiwan University and colleagues highlight a problem with these methods, indicating that switching the pointing directions of an antiferromagnet's spins—a requirement for their use in devices—with all-electrical methods might be more difficult than researchers thought [1].

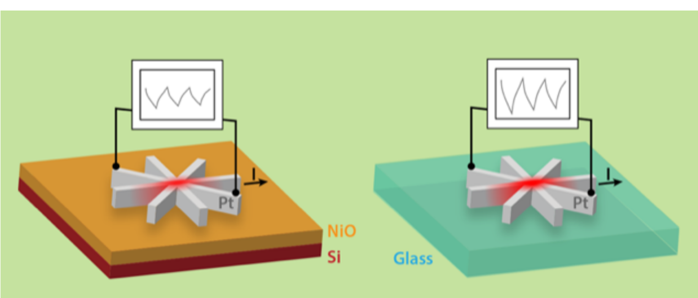

Figure 1: (Left) Platinum (Pt) strips grown on antiferromagnetic nickel oxide (NiO) films convert charge current to spin current, which is intended to switch the pointing direction of the insulating NiO's spins. The switching is observed via a sawtooth voltage pattern. However, the Pt heats dramatically when the current is applied and (right) this heating reproduces the sawtooth pattern even when no antiferromagnet is present. (APS/Alan Stonebraker)

*Department of Physics and Astronomy, University of Denver, Denver, CO, USA

From the first iPod that stored music to today's server farms that house the world's many cat videos, the spins of ferromagnets—which encode data's 1's and 0's as domains of up- and down-pointing spins—have been key to making usable devices for storing information. The success of this technology has led researchers to ask whether spin might also be utilized for processing information. To achieve that, so-called spintronic circuits, which can carry spin currents, would likely need to become smaller, more stable, and faster than they are today. That is where antiferromagnetic materials come in. For data storage, their pattern of alternating spins reduces the impact of stray or nearby magnetic fields, potentially reducing data loss by making their bits more stable. For spin transport, the antiferromagnetic order of the spins should increase the maximum speed at which a spin wave can carry magnetic information through the material, allowing devices made from antiferromagnets to operate faster than those made from ferromagnets.

Several recent advances have brought antiferromagnets closer to practical use. In 2014, researchers demonstrated spin transport through an insulating antiferromagnet. The achievement could allow for faster and more energy efficient devices than current devices made from metals or semiconductors, as running a spin current through an insulator causes less heating [2]. More critically, in 2016, researchers discovered a simple way to electrically "switch" an antiferromagnetic bit [3]. Switching involves rotating the axes of the spins by some angle and is important for writing data.

To electrically switch a magnetic domain, one injects a current of conduction electrons. The intrinsic angular momentum, or spin, of these electrons interacts with the orbital angular momentum of the atoms in the material, generating a flow of spins called a spin current. If this spin current is absorbed by the magnetic domain it causes a torque that can switch the domain. This switching mechanism is therefore called spin-orbit torque (SOT) switching. SOT switching is a powerful tool for manipulating ferromagnets [4], and there are many tools for confirming a switch in these materials.

The same is not true for antiferromagnets, where proving that a bit has switched turns out to be more difficult. To observe the switching in metallic antiferromagnets the authors of Ref. [3] adapted an electrical measurement that is sensitive to the ordering of the material's spins. Specifically, they applied a series of large current pulses to the metallic antiferromagnet with consecutive pulses flowing in opposite directions. Switching was then monitored via the voltage induced by the planar Hall effect. A sawtooth pattern in the voltage was taken as confirmation of antiferromagnetic switching.

Very shortly after this groundbreaking work on a metallic antiferromagnet, research groups across the globe applied the technique to antiferromagnetic insulators, such as nickel oxide (NiO). In these experiments, the insulator is interfaced to a metallic layer, most often platinum (Pt). A charge current in the Pt generates a spin current that can flow into the NiO and switch regions of the antiferromagnet's spins. Researchers initially relied on the same electrical detection scheme used for metallic antiferromagnets, and indeed they saw the characteristic sawtooth pattern. But the new work demonstrates that this key electrical signature can also be generated in a device with no magnetic components at all, leading to questions about the technique's efficacy for detecting switching.

Chiang and colleagues started by depositing 4-nm-thick Pt strips in a star configuration on top of a 60-nm-thick NiO film grown on a silicon substrate (Fig. 1). This device reproduced those commonly used for Pt/NiO SOT switching experiments. Applying charge current pulses of about 30 mA that were intended to generate spin currents that would reorient the NiO's spins, the team observed the characteristic sawtooth voltage pattern. In a second device, the researchers replaced the silicon with glass, a poor conductor of heat, and observed a large increase in the magnitude of the sawtooth voltage. This result is unexpected, since the NiO layer was nominally similar in both experiments. Finally, in a third device they deposited the Pt directly on glass, removing the magnetic material entirely (Fig. 1). The sawtooth signal remained and had an even larger magnitude than either of the signals detected for the other two devices. This dramatic result clearly shows that the electrical signal observed in these experiments cannot be evidence of switching of the insulating antiferromagnet.

Using computer models, Chiang and colleagues make a strong case that the sawtooth voltage pattern is instead caused by heat generated in the Pt strips. This heat drives thermoelectric voltages that persist for surprisingly long periods of time, even up to one hour. The warmed Pt and the resulting thermal gradients that develop between the various Pt strips depend on the heat conductivity of the underlying substrate, which is why glass, with its low heat conductivity, causes larger voltages. Thermal gradients of this sort frequently arise in spintronic devices and offer challenges and opportunities in their use [5].

Questions remain regarding the details of the physical mechanism generating the sawtooth signals, which could involve electromigration—the transport of electrons due to the presence of an electric field. Chiang *et al.*'s work raises concerns that we must resolve to realize spintronic devices based on insulating antiferromagnets. However, the researchers may paint with too broad a brush when they question whether SOT switching has been demonstrated in antiferromagnets at all. This concern ignores a good deal of evidence in favor of antiferromagnetic switching, including the demonstration of a memory element using CuMnAs, a metallic antiferromagnet [6], and of imaging techniques that show modification of antiferromagnetic domains in response to charge currents [7–12]. Techniques ranging from synchrotron x-ray measurements to novel thermal scanning probe microscopy have also provided clear proof of switching in both metallic and insulating antiferromagnets, though never with the uniform domain reversal seen in ferromagnets [4]. All of these other techniques are much slower to implement than electrical ones, so measurements are made long after the heating caused by "writing" currents has dissipated.

Chiang *et al.*'s work could explain a puzzling aspect of the switching experiments. A large voltage signal is often detected from what imaging techniques show is quite minor realignment of the antiferromagnetic domain pattern. Perhaps the nonmagnetic heating effect that Chiang and colleagues observe provides the signal's origin. If so, that would potentially resolve this mystery. The team also highlights a number of other puzzles that need to be solved to continue progress in the field. For example, does an antiferromagnetic film that is only a few nanometers thick have the same spin structure as the bulk material? Do the different interfaces, which arise from varying the substrate, modify the spin-orbit coupling throughout the film stack? Perhaps most importantly, does an artifact-free electrical method exist for detecting antiferromagnetic switching in insulators? These questions highlight the difficulty in harnessing antiferromagnets, but answering them could yet put antiferromagnets to very practical use.

This research is published in *Physical Review Letters*.

REFERENCES

[1] C. C. Chiang, S. Y. Huang, D. Qu, P. H. Wu, and C. L. Chien, "Absence of evidence of electrical switching of the antiferromagnetic Néel vector," Phys Rev. Lett. **123**, 227203 (2019).

[2] H. Wang, C. Du, P. C. Hammel, and F. Yang, "Antiferromagnonic spin transport from $Y_3Fe_5O_{12}$ into NiO," Phys. Rev. Lett. **113**, 097202 (2014).

[3] P. Wadley *et al.*, "Electrical switching of an antiferromagnet," Science **351**, 587 (2016).

[4] A. Manchon, J. Železný, I. M. Miron, T. Jungwirth, J. Sinova, A. Thiaville, K. Garello, and P. Gambardella, "Current-induced

spin-orbit torques in ferromagnetic and antiferromagnetic systems,'' Rev. Mod. Phys. **91**, 035004 (2019).

[5] C. H. Back, G. E. W. Bauer, and B. L. Zink, ''Special issue on spin caloritronics,'' J. Phys. D. Appl. Phys. **52**, 230301 (2019).

[6] K. Olejník *et al.*, ''Antiferromagnetic CuMnAs multi-level memory cell with microelectronic compatibility,'' Nat. Comun. **8**, 15434 (2017).

[7] M. J. Grzybowski *et al.*, ''Imaging current-induced switching of antiferromagnetic domains in CuMnAs,'' Phys. Rev. Lett. **118**, 057701 (2017).

[8] P. Wadley *et al.*, ''Current polarity-dependent manipulation of antiferromagnetic domains,'' Nat. Nanotech. **13**, 362 (2018).

[9] S. Yu. Bodnar, M. Filianina, S. P. Bommanaboyena, T. Forrest, F. Maccherozzi, A. A. Sapozhnik, Y. Skourski, M. Kläui, and M. Jourdan, ''Imaging of current induced Néel vector switching in antiferromagnetic Mn_2Au,'' Phys. Rev. B **99**, 140409R (2019).

[10] T. Moriyama, K. Oda, T. Ohkochi, M. Kimata, and T. Ono, ''Spin torque control of antiferromagnetic moments in NiO,'' Sci. Rep. **8**, 14167 (2018).

[11] L. Baldrati *et al.*, ''Mechanism of Néel order switching in antiferromagnetic thin films revealed by magnetotransport and direct imaging,'' Phys. Rev. Lett. **123**, 177201 (2019).

[12] I. Gray *et al.*, ''Spin Seebeck imaging of spin-torque switching in antiferromagnetic Pt/NiO heterostructures,'' Phys. Rev. X **9**, 041016 (2019).

10.1103/Physics.12.134

